Data Fusion in a Multistatic Radar System

Pietro Stinco, Maria Greco, Fulvio Gini

Abstract— **This paper deals with the design and performance evaluation of a multistatic radar system where target detection is performed by jointly combining the signals arising from multiple spatially dispersed transmitters and receivers.**

We provide some simulation results that illustrate how significant improvements in radar system performances can be achieved by exploiting the Ambiguity Function as tool for determining the target resolution capability of each channel of the multistatic system.

Index Terms— **Multistatic system, Ambiguity Function, Fisher Information, Cramér-Rao lower bound, Multistatic detector.**

I. Introduction

Multistatic radars utilize multiple transmitters and receivers. Such systems differ from typical modern active radars since they consist of several different monostatic and bistatic channels of observation. Due to this spatial diversity, these systems present challenges in managing their operation as well as in usefully combining the data from multiple sources of information on a particular area of surveillance. The information gain, obtained through this spatial diversity, combined with some level of data fusion, can give rise to a number of advantages over both the individual monostatic and bistatic cases for typical radar functions, such as detection, parameter estimation, tracking and identification.

As widely known, the performance of each channel of the multistatic system heavily depends on the transmitted waveform and on the geometry of the scenario, that is, the position of receivers and transmitters with respect to the position of the target. Both geometry factors and transmitted waveforms play an important role in the shape of the Ambiguity Function [2], which is often used to measure the possible global resolution and large error properties of the target parameters estimates.

Exploiting the relation between the Ambiguity Function and the Cramér-Rao Lower Bound (CRLB) [1], it is possible to calculate the bistatic CRLBs of target range and velocity of each TX-RX pair as a function of the target kinematic parameters and to provide a local measure of the estimation accuracy of these parameters [4], [5].

In this work, we exploit the results obtained from this analysis to compute the rules for selecting the best weighting coefficients for fusing the signals from multiple receivers in order to improve the detection performance and the estimation accuracy of the kinematic parameters of the target.

P. Stinco, M. Greco and F. Gini are with Department of "Ingegneria dell'Informazione", University of Pisa, Via G. Caruso 16 – Pisa, 56122, Italy (phone: +39 050 2217578; e-mail: pietro.stinco@iet.unipi.it).

II. Channel Performance Evaluation

In the most general case, a Multistatic radar system is composed of M transmitters and N receivers, co-located or not, surveying a common coverage area. Supposing that a set of orthogonal waveform is transmitted, where orthogonality is assumed to be maintained for any Doppler-delay shift, with proper design, it is possible to separate each transmit-receive path, so that each sensor can receive echoes due the signals generated by all the transmitters and can select the transmitted signal of interest. In this way, the multistatic system can be considered as consisting of NM different monostatic and bistatic channels of observation.

The performance of each channel clearly depends on the transmitted waveform but unfortunately is also heavily sensitive to the geometry, that is the position of the receiver and the transmitter with respect to the target. In the context of radar, one of the most known key tool for determining target resolution capability is the Complex Ambiguity Function (CAF). The CAF is a consequence of the nature of the optimal detector, which involves decision-making based on the output of a matched filter determined from the transmitted waveform.

As a matter of fact, the Complex Ambiguity Function is the auto-correlation of the complex envelope of the transmitted waveform with a copy shifted in time and frequency, and presents the point target response of the waveform as a two-dimensional function of delay and Doppler, showing the resolution, sidelobe structure and ambiguities in the delay and Doppler domains.

The mathematical definition of the CAF is [2]:

$$X(\tau_H,\tau_a,\nu_H,\nu_a)=\int_{-\infty}^{+\infty}u(t-\tau_a)u^*(t-\tau_H)e^{-j2\pi(\nu_H-\nu_a)t}dt \quad (1)$$

where $u(t)$ is the complex envelope of the transmitted signal, τ_a and ν_a are the actual delay and Doppler frequency of the radar target respectively and τ_H and ν_H are the hypothesized delay and frequency. In the monostatic case there is a linear relationship between τ_a and ν_a, and the range position R_a and radial velocity V_a of the target, more specifically $\tau_a = 2R_a/c$ and $\nu_a = 2V_a f_C/c$, where f_C is the carrier frequency of the reference signal $u(t)$ and c is the speed of light. Similar relations hold for τ_H and ν_H.

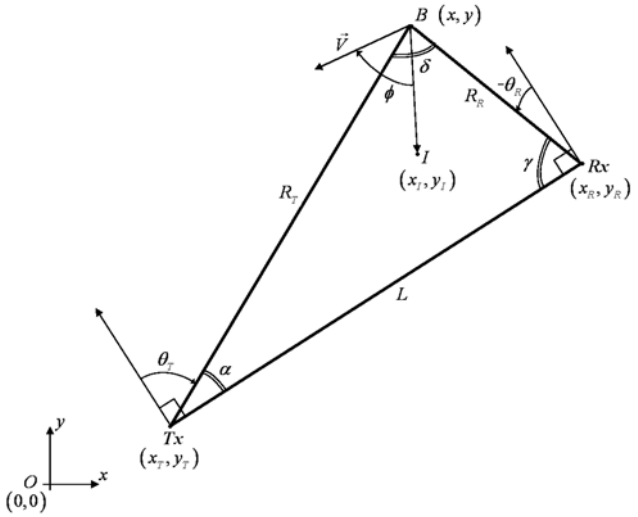

Fig 1 Bistaic Geometry

The Ambiguity Function (AF) is defined as the absolute value of the CAF and, clearly, it is maximum for $\tau_H = \tau_a$ and $v_H = v_a$. The AF directly determines the capability of a system to resolve two targets that exist at different ranges from the radar and have different radial velocities. When the receiver signals from the target have similar energy, the resolution is equal to the half power width of the AF mainlobe.

The AF is also related to the accuracy with which the range and the velocity of a given target can be estimated. The CRLBs on estimation accuracy are dependent on both the *SNR* and the second derivatives of the AF, that is the sharpness of the AF mainlobe.

More generally, the information that can be extracted from the echo of a radar waveform can be quantified in terms of Fisher information. In the monostatic configuration the Fisher Information Matrix (FIM) can be calculated from the following relationship [1], [3]:

$$\mathbf{J}_M(\tau_a,v_a) = -2SNR\left[\begin{array}{cc} \dfrac{\partial^2|X(\tau,v)|}{\partial\tau^2} & \dfrac{\partial^2|X(\tau,v)|}{\partial\tau\partial v} \\ \dfrac{\partial^2|X(\tau,v)|}{\partial v\partial\tau} & \dfrac{\partial^2|X(\tau,v)|}{\partial v^2} \end{array}\right]_{\tau=0,v=0} \quad (2)$$

where $\tau = \tau_H - \tau_a$ and $v = v_H - v_a$.

The AF is at the heart of this expression since it is the log-likelihood function excluding the effect of signal attenuation and clutter.

The inverse of the FIM is the Cramér-Rao lower bound which bounds the error variance of the estimates produced from the radar measurements. In particular, we have:

$\mathrm{CRLB}(\tau_a) = \left[\mathbf{J}_M^{-1}(\tau_a,v_a)\right]_{1,1}$ and $\mathrm{CRLB}(v_a) = \left[\mathbf{J}_M^{-1}(\tau_a,v_a)\right]_{2,2}$.

This is useful because it gives an indication of the best achievable performance, independent of the filtering algorithm. In monostatic configuration, estimation of the time delay and Doppler shift directly provides information on range and velocity of the target. This is possible also in the case of bistatic radar configuration, even if the relation between measured or estimated time delay and Doppler frequency, and target distance and velocity is not linear.

In particular, to obtain the expression of the Bistatic Ambiguity Function (BAF), we must replace τ_H and v_H in (1) with the following:

$$\tau_H = \frac{R_R + \sqrt{R_R^2 + L^2 + 2R_R L\sin\theta_R}}{c} \quad (3)$$

$$v_H = 2\frac{f_C}{c}V_B\sqrt{\frac{1}{2} + \frac{R_R + L\sin\theta_R}{2\sqrt{R_R^2 + L^2 + 2R_R L\sin\theta_R}}} \quad (4)$$

where, referring to the generic bistatic configuration of Figure 1, R_R is the range from receiver to target, L is the baseline between the transmitter and the receiver, θ_R is the look angle of the receiver and V_B is the component of the target velocity in the direction of the bistatic bisector, i.e. the bisector of the angle at the vertex of the bistatic triangle which represents the target.

In the above equations we used the cosine law relation $R_T^2 = R_R^2 + L^2 + 2R_R L\sin\theta_R$, which gives the range from transmitter to target R_T, as a function of the range from receiver to target and the look angle of the receiver.

In the bistatic configuration we should express the ambiguity function in terms of the bistatic $\tau(R_R,\theta_R,L)$ and $v(R_R,V_B,\theta_R,L)$, and derive it with respect to the useful parameters R_R and V_B, as follows:

$$\mathbf{J}_B(R_R,V_B) = -2SNR\left[\begin{array}{cc} \dfrac{\partial^2|X(R_R,V_B)|}{\partial R_R^{\,2}} & \dfrac{\partial^2|X(R_R,V_B)|}{\partial R_R\partial V_B} \\ \dfrac{\partial^2|X(R_R,V_B)|}{\partial V_B\partial R_R} & \dfrac{\partial^2|X(R_R,V_B)|}{\partial V_B^{\,2}} \end{array}\right]_{R_R=R_a,V_B=V_a} \quad (5)$$

Using the derivative chain rule and letting $R_R = R_a$ and $V_B = V_a$, after some algebra it is possible to verify that [4],[5]:

$$\mathbf{J}_B(R_R,V_B) = \mathbf{P}\mathbf{J}_M(\tau_a,v_a)\mathbf{P}^T \quad (6)$$

where

$$\mathbf{P} = \left[\begin{array}{cc} \dfrac{\partial\tau}{\partial R_R} & \dfrac{\partial v}{\partial R_R} \\ \dfrac{\partial\tau}{\partial V_B} & \dfrac{\partial v}{\partial V_B} \end{array}\right] \quad (7)$$

From the last equation it is clearly apparent that the local accuracy in the bistatic case depends not only on the transmitted waveform but also on the bistatic geometry.

For $L=0$ the bistatic CRLBs coincide with the monostatic CRLBs.

As an example, let consider the case in which the transmitted signal is a sequence of linear frequency modulated (LFM) pulses or chirps.

The complex envelope of the transmitted unitary power

signal is then given by:

$$u(t)=\frac{1}{\sqrt{N_p}}\sum_{n=0}^{N_p-1}u_1\left(t-nT_R\right) \tag{8}$$

where

$$u_1(t)=\begin{cases}\frac{1}{\sqrt{T}}\exp\left(j\pi kt^2\right) & 0\le t\le T\\ 0 & elsewhere\end{cases} \tag{9}$$

N_p is the number of pulses, T_R is the burst repetition time and T is the duration of each pulse, with $T<T_R/2$. Moreover, $kT^2=BT$ is the effective time-bandwidth product of the signal and B is the total frequency deviation. Based upon the definition (1) we can calculate the monostatic complex ambiguity function for the signal $u(t)$ in (8) and (9) as [4]:

$$X(\tau,\nu)=\begin{cases}\frac{1}{N_p}\sum_{p=-(N_p-1)}^{(N_p-1)}A_p(\tau,\nu)B_p(\tau,\nu)C_p(\nu) & |\tau|<N_pT_R\\ 0 & elsewhere\end{cases} \tag{10}$$

where

$$A_p(\tau,\nu)=\exp\left[j\pi\nu(N_p-1+p)T_R\right]\left(1-\frac{|\tau-pT_R|}{T}\right) \tag{11}$$

$$B_p(\tau,\nu)=\frac{\sin\left[\pi T\left(\nu-k\left(\tau-pT_R\right)\right)\left(1-|\tau-pT_R|/T\right)\right]}{\pi T\left(\nu-k\left(\tau-pT_R\right)\right)\left(1-|\tau-pT_R|/T\right)} \tag{12}$$

$$C_p(\nu)=\frac{\sin\left[\pi\nu\left(N_p-|p|\right)T_R\right]}{\sin\left(\pi\nu T_R\right)} \tag{13}$$

After some algebra, it is also possible to verify that, in the monostatic configuration, the FIM is [4]

$$\mathbf{J}_M\left(\tau_a,\nu_a\right)=-2SNR\begin{bmatrix}-\frac{k^2\pi^2T^2}{3} & \frac{k\pi^2T^2}{3}\\ \frac{k\pi^2T^2}{3} & -\frac{\pi^2T^2}{3}+\frac{\pi^2T_R^2(1-N_p{}^2)}{3}\end{bmatrix} \tag{14}$$

Using this result, combined with (6) and (7), it is possible to compare the monostatic and the bistatic Root Cramér-Rao Lower Bounds (RCRLBs). Figure 2-4 show the RCRLBs of range and velocity, both in the monostatic and bistatic case, obtained selecting T=250μsec, T_R= 1msec, B= 1MHz, f_C=10GHz and N_p = 8. In particular, Figure 2 shows the RCRLBs as a function of the receiver to target range R_R when θ_R =0. While Figure 3 shows the results obtained choosing θ_R = -0.49π. Figure 4 shows the RCRLBs as a function of the receiver look angle θ_R, both in the case of $R_R<L$ and $R_R>L$. All these figures have been obtained choosing V_B=250 m/sec, L=50km and holding constant the SNR to 0dB. It is evident that, for all the parameter values we tested, the bistatic RCRLBs are always higher than the monostatic RCRLBs. The bistatic RCRLBs get even worse when the target approaches the baseline, that is when $R_R\le L$ and θ_R approaches $-\pi/2$.

In this case, the resulting delay is L/c and the radial velocity is zero, therefore resolution is totally lost and the RCRLBs tend to infinity. This can be appreciated by realizing that the

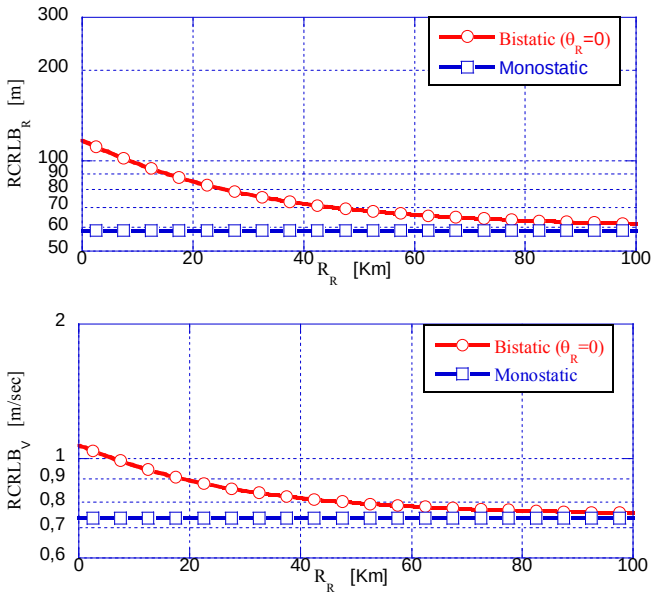

Fig 2 RCRLB of Range and Velocity as a function of receiver to target range R_R, θ_R=0; L=50km, SNR=0dB.

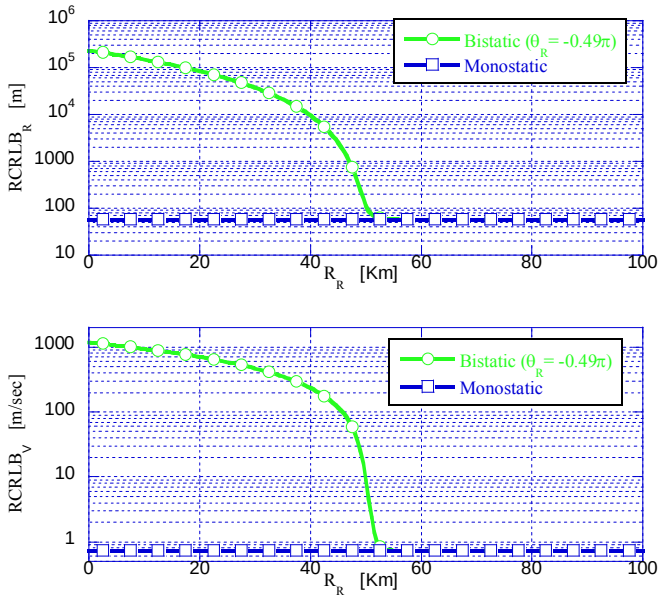

Fig 3 RCRLB of Range and Velocity as a function of receiver to target range R_R, θ_R= -0.49π; L=50km, SNR=0dB.

echo arrives at the receiver at the same instant as the direct signal, independent of the target location, and the Doppler shift of a target crossing the bistatic baseline must be zero, because the transmitter-to-target range changes in an equal and opposite way to the target-to-receiver range, independent of the magnitude and direction of the target velocity. However, the effects of the bistatic geometry are less prominent when the distance to the target increases; in this case the bistatic system behaves more and more as a monostatic system.

The results derived in this Section can be used for defining a tool to evaluate the performance of a given monostatic or bistatic channel of the multistatic system and for design multistatic weighting coefficients for the detection process

that will be described in the next Section.

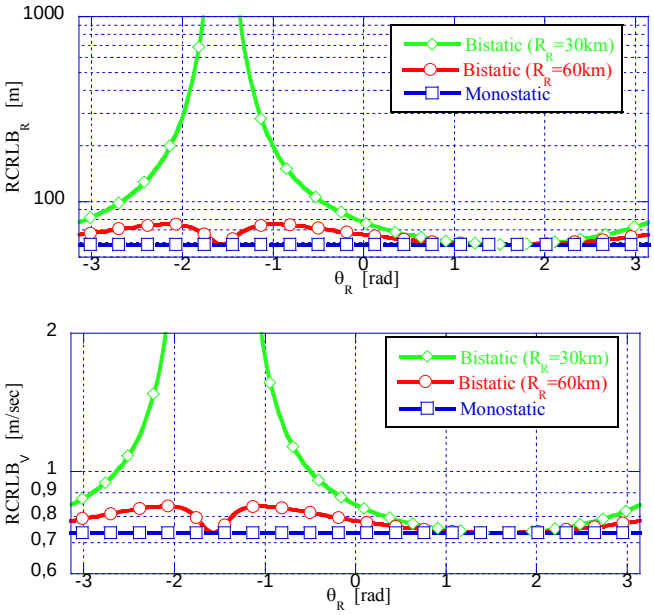

Fig 4 RCRLB of Range and Velocity as a function of receiver look angle θ_R; L=50km, SNR=0dB.

III. Fusion Process

The purpose of this section is to evaluate the performance of the Multistatic Detection algorithms. In our approach the processing concerning the detection is shared among the receivers and the central processor. In particular, the Multistatic Detector refers to a centralized nomenclature where the data at each receiver are first collected by a central processor and then jointly combined for the detection. So, the decision process is separated into two steps, the local processing at each receiver to perform matched filtering and the central processing to perform the fusion of the collected data and to compare the result with a proper threshold. It is assumed that the central processor knows the geometry of the multistatic scenario, that is, the position of each transmitter and each receiver. In this way, for each point (x,y,V_x,V_y) of the surveillance map, the central processor is able to select the corresponding range-velocity cell of each receiver.

For ease of notation and without lack of generality here it is assumed that the multistatic system is composed of a single transmitter and N receivers, thus, the problem of detecting a target signal in a fixed resolution cell of the surveillance map can be posed in terms of the following binary hypotheses test:

$$\begin{cases} r_i = \alpha_i c_i + n_i & H_1 \\ r_i = n_i & H_0 \end{cases} \quad i=1,\ldots,N \tag{15}$$

where the sample r_i is the output of the filter matched to the normalized transmitted signal for the i-th receiver in the range-velocity cell corresponding to the point (x,y,V_x,V_y) which is probed to ascertain the presence of a target. Note that if the transmitted signal is a burst of pulses, the sample r_i is the output of the filter matched to entire burst. In the signal model in eq. (15), n_i is the additive noise at the i-th sensor; it is modelled as a zero-mean complex Gaussian variable, in short $n_i \sim CN(0, \sigma^2)$. The samples n_i are assumed to be independent from channel to channel and identically distributed. The parameter α_i accounts for the channel propagation effect and the target radar cross section. We considered the case in which the amplitude α_i is a random variable. It depends on the target bistatic RCS of the i-th bistatic angle. This, together with the mentioned features of the multistatic geometry, justifies the assumption that the α_is are mutually independent random quantities. With regard to the marginal PDFs, α_i is a zero-mean complex Gaussian variable with variance σ_i^2 varying from path to path $\alpha_i \sim CN(0, \sigma_i^2)$. In particular the Signal to Noise power Ratio at the input of the i-th channel is defined as

$$SNR_i = \frac{\sigma_i^2}{\sigma^2} = \frac{Const}{\left(R_T^{(i)} R_R^{(i)}\right)^2} \tag{16}$$

and, as mentioned, is inversely proportional to the path loss factor $(R_T^{(i)}R_R^{(i)})^2$ due to propagation where, $R_T^{(i)}$ and $R_R^{(i)}$ are the range from transmitter to target and the range from receiver to target for the i-th channel, respectively. The parameter c_i is a complex number with absolute value lower than or equal to one which accounts for the other effects of propagation and scattering along the i-th path. The meaning of c_i will be discussed later on, for the moment let consider the case in which c_i=1. With this assumption and considering that the amplitude α_i and the noise n_i are independent, the observation r_i is a zero-mean complex Gaussian variable under both hypotheses. Therefore, it is possible to write:

$$\begin{cases} r_i \sim CN\left(0, \sigma_i^2 + \sigma^2\right) & H_1 \\ r_i \sim CN\left(0, \sigma^2\right) & H_0 \end{cases} \quad i=1,\ldots,N \tag{17}$$

Hence, by exploiting the independence of individual likelihoods in each channel, it is possible to verify that the Neyman-Pearson decision test develops into the following form [7],[8]:

$$\sum_{i=1}^{N} p_i \left|r_i\right|^2 \underset{H_1}{\overset{H_0}{\lessgtr}} \lambda \tag{18}$$

where

$$p_i = \frac{SNR_i}{1+SNR_i} \tag{19}$$

The obtained receiver is shown in Figure 5 where there are the two steps of the decision process: the local processing and the central processing. Note that the weight p_i are non negative and are an increasing function of SNR_i, therefore the central processor emphasizes those channels along which the SNRs are the highest. Note that the receiver to implement the given test, depending on cell under test of the surveillance map, needs to continually update the weights, which are themselves dependent, through SNR_i, on the distances from the transmitter to the target and from the target to the receiver.

Consider now the case in which, under the H_1 hypothesis c_i

in eq. (15) is a complex random variable. This simple assumption has been done in order to model the effects of the bistatic geometry along the *i*-th path. In particular we generated c_i as

$$c_i = X(\tau_i, v_i) \tag{20}$$

where $\tau_i = \tau_{Hi} - \tau_a$ and $v_i = v_{Hi} - v_a$ are the delay and Doppler shift for the *i*-th path obtained using eqs. (3)-(4) and by random generating the estimates of the range and velocity as

$$\hat{R}_R^{(i)} \sim N(R_R^{(i)},\ \mathrm{CRLB}_R^{(i)}) \tag{21}$$

$$\hat{V}_B^{(i)} \sim N(V_B^{(i)},\ \mathrm{CRLB}_V^{(i)}) \tag{22}$$

where $R_R^{(i)}$ and $V_B^{(i)}$ are the actual range and bistatic velocity of the target, while $\mathrm{CRLB}_R^{(i)}$ and $\mathrm{CRLB}_V^{(i)}$ are the Cramér-Rao lower bounds of range and velocity in the *i*-th path. By random generating $\hat{R}_R^{(i)}$ and $\hat{V}_B^{(i)}$, the value of c_i takes into account the mis-matching at the *i*-th receiver, moreover, due the geometry dependent non linear transformation of eqs (3) and (4), the value of c_i takes also into account the effects of the distortion of the Ambiguity Function due to the bistatic geometry. As an example, consider the case in which $\mathrm{CRLB}_R^{(i)}$ and $\mathrm{CRLB}_V^{(i)}$ are low, in this case the values assumed by $\hat{R}_R^{(i)}$ and $\hat{V}_B^{(i)}$ are near the actual range and velocity, therefore the values assumed by τ_i and v_i are almost zero, and hence the value assumed by c_i is near the maximum that is 1. On the other hand, for a bad bistatic geometry, the values assumed by $\mathrm{CRLB}_R^{(i)}$ and $\mathrm{CRLB}_V^{(i)}$ are very high, therefore there is a high probability that also τ_i and v_i are high and hence the value assumed by them is almost zero and the observed signal is only noise. In other words, by generating in this way the value of c_i, the signal model in eq (15) is now dependent on the sharpness of the CAF around its maximum and to the distortion of its behaviour due to the bistatic geometry. It is clearly apparent that it is very difficult to derive the PDF of c_i and hence it is difficult to derive the Neyman-Pearson decision test. By the way, our approach is to use the same receiver of eq. (18) and shown in Figure 5 but choosing the weights p_i in a different manner. In fact, the weights in eq. (19) depends only on the energy path loss and they do not take into account the other effects due to the bistatic geometry. As an example, let consider the case of a target is in the baseline between the transmitter and the *i*-th receiver. When the distance between the transmitter and *i*-th receiver is low, the expected SNR is high and therefore the central processor using the weights in (19) tends to emphasize this path during the detection process. As shown, in this case the resolution is totally lost and therefore the observations from this path can significantly degrade the performance of the whole system. Therefore, the rule for selecting the weighting coefficients should be different. In particular, the weights should be highlight those channels that exhibit the best performance in terms of estimation accuracy of the target parameters instead of emphasizes those along which the *SNR*s are the highest.

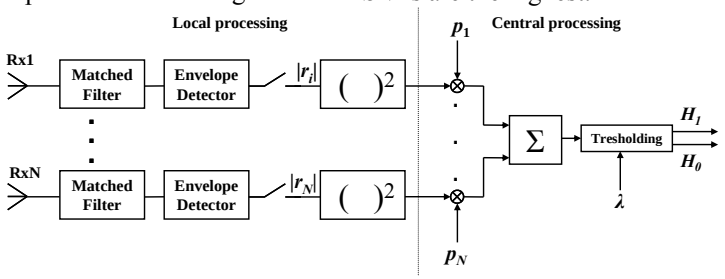

Fig 5 Flow diagram of the multistatic detector

In this work we propose the following weighting rule

$$p_i = \frac{Trace\left\{\mathbf{J}_B^{-1}\left(R_R^{(i)}, V_B^{(i)}\right)\right\}^{-1}}{\gamma + Trace\left\{\mathbf{J}_B^{-1}\left(R_R^{(i)}, V_B^{(i)}\right)\right\}^{-1}} \tag{23}$$

where $Trace\{\bullet\}$ is the trace operator and γ is a constant that we fixed equal to the inverse of the sum of the CRLBs of range and velocity in the monostatic case when *SNR*=0dB. It is important to recall that $R_R^{(i)}$ and $V_B^{(i)}$ are the actual range and velocity of the target. Therefore, depending on the cell (x,y,V_x,V_y) under test, the central processor can easily calculate these two values for each channel knowing the position of each sensor of the multistatic system.

As apparent in eq. (23), the weights p_i depend on the inverse of the bistatic Fisher Information Matrix which is dependent on the energy path loss through SNR_i, on the geometry and also on the transmitted waveform. This is also important in the case of a multistatic system where multiple transmitters are used. Using the weights in (23) the central processor emphasizes those channels that exhibit the best performance in terms of estimation accuracy and is also able to discard those channels where the resolution is totally lost. In this case the trace of the inverse of the bistatic FIM tends to infinity and the therefore the weight p_i tends to zero. Figure 6 shows the multistatic scenario analyzed in our simulations. The multistatic system is composed of one transmitter and three receivers. The distance between the transmitter and each receiver is the same and equal to 30km.

The value of *Const* in eq. (16) is 186 dBm^4, in this case if $R_T = R_R$= 141km the expected SNR is -20 dB. As shown in Figure 6, in our simulation we considered three cases. In the first one we considered a target in the middle of the first baseline, that is between the transmitter and the first receiver. In this case the target is moving with a speed of 250 m/sec and direction of 135° with respect to the horizontal axis. In the second case the target is in the second baseline, 10 km far from the transmitter, moving with a speed of 250 m/sec and direction of 150°. While in the third case, the target is 15 km far from the third baseline and 20 km far from the second baseline, and it is moving with a speed of 250 m/sec and direction of 180° with respect to the horizontal axis. Table 1 shows the weighting coefficients obtained with both the methods, that is the "*SNR*" rule in eq. (19) and the "*Trace*" rule in eq. (23). Note that the coefficients have been

normalized in order to satisfy the relationship $\Sigma p_i=1$.

As apparent from Figure 6, in Case 1 the target is in the first baseline, therefore the resolution of the first receiver is totally lost also if the SNR for this path is the highest. As apparent from Table 1, the coefficient corresponding to the first receiver is null using the Trace rule while it is the highest using the SNR rule. Similar considerations can be drawn for Case 2. In the third case the target is in an optimal position for all the receiver, the main difference from one receiver to the other is related only to the energy path loss, therefore the weighting coefficients obtained with both the rule are almost the same.

Figure 7 shows the Receiver Operating Characteristic (ROC) of the multistatic detector in eq. (18) for all the three analyzed cases. We also plotted the ROC obtained by forcing all the coefficients to $1/N$. As apparent from the results the ROC obtained in Case 3 (dash-dotted lines) are almost the same for the three weighting rules, while in Case 1 (solid lines) and Case 2 (dashed-lines) the performances obtained with the Trace rule are the best. Moreover, in Case 1, the performance obtained with the SNR rule is lower than that obtained with all the weights equal to $1/N$. In this case, the SNR for the first receiver is the highest but, due to bad geometry, the resolution is totally lost. Using the SNR rule, the central processor emphasizes the observations from the first sensors and this strongly degrades the performance of the multistatic detector.

IV. Conclusions

In this work we evaluated the performance of a Multistatic Detection algorithm. The analyzed detector refers to a centralized nomenclature where the data at each receiver are first collected by a central processor and then jointly combined using proper weights for the detection. Usually, the weighting coefficients are an increasing function of the expected SNR. However, in a multistatic radar system the performance of each bistatic channel heavily depends upon the geometry which plays an important role in the shape of the bistatic ambiguity function. Therefore, depending on the geometry, it is also possible that in channel with a high SNR the estimation accuracy of the target parameters is very low.

In this work we proposed a rule for obtain the weighting coefficients that depends on the FIM which is itself dependent on the SNR, the AF and therefore on the geometry and the transmitted waveform.

From simulation results, we showed that it is possible to improve the performance of the multistatic detector using the proposed technique. The obtained results can serve as a guideline for future multistatic fusion rule development.

TABLE I
Weighting Coefficients

	SNR	TRACE
Case 1	**p**=[0.3495; 0.3328; 0.3177]	**p**=[0.0000; 0.4984; 0.5016]
Case 2	**p**=[0.3317; 0.3366; 0.3317]	**p**=[0.5000; 0.0000; 0.5000]
Case 3	**p**=[0.2735; 0.3553; 0.3712]	**p**=[0.2939; 0.3449; 0.3612]

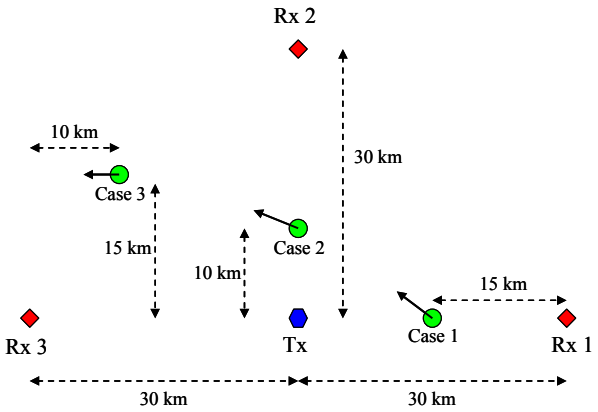

Fig 6 Simulated scenario

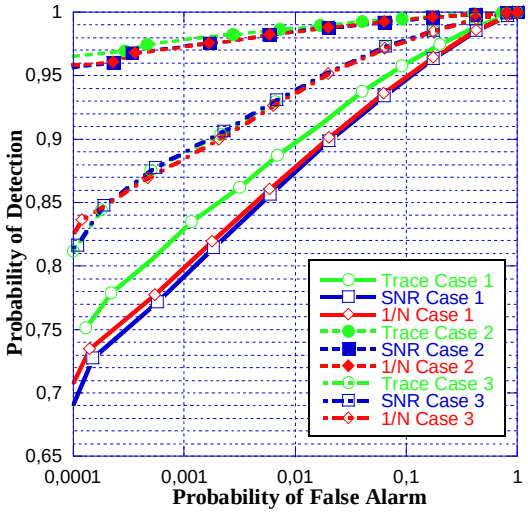

Fig 7 Receiver Operating Characteristic of the Multistatic Detector.

References

[1] H. L. Van Trees, Detection, Estimation and Modulation Theory. New York: Wiley, 1971, Vol. III.

[2] T. Tsao, M. Slamani, P. Varshney, D. Weiner, H. Schwarzlander, "Ambiguity Function for a Bistatic Radar", *IEEE Trans. on AES*, Vol. 33, No. 3, July 1997, pp. 1041-1051.

[3] A. Dogandzic, A. Nehorai, "Cramér-Rao Bounds for estimating Range, Velocity, and Direction with and Active Array", *IEEE Trans. on SP*, Vol. 49, No. 6, June 2001, pp. 1122-1137.

[4] A. Farina, F. Gini, M. Greco, P. Stinco and L. Verrazzani, "Optimal Selection of the TX-RX Pair in a Multistatic Radar System", *COGIS'09*, Paris, France, November 2009.

[5] M.Greco, P. Stinco, F. Gini, M. Rangaswamy, "Cramér-Rao Bounds and TX-RX Selection in a Multistatic Radar Scenario (invited)", *IEEE Int. Radar Conf. 2010*, Washington DC, USA, 10-14 May 2010.

[6] I. Bradaric, G.T. Capraro, D. D. Weiner, and M. C. Wicks, "Multistatic Radar Systems Signal Processing," *2006 IEEE Radar Conference*, Verona, New York, USA, April, 2006.

[7] D'Addio, E.; Farina, A.; , "Overview of detection theory in multistatic radar," Communications, *IEE Proc F*, vol.133, no.7, pp.613-623, December 1986

[8] E. Conte; E. D'Addio; A. Farina; M. Longo , "Multistatic radar detection: synthesis and comparison of optimum and suboptimum receivers," Communications, *IEE Proc F*,, vol.130, no.6, pp.484-494, October 1983

[9] I. Papoutsis, C.J. Baker, and H.D. Griffiths, "Netted Radar and the Ambiguity Function," *IEEE Int. Radar Conf.*, Washington DC, 2005.

[10] Derham, T.; Doughty, S.; Baker, C.; Woodbridge, K.; , "Ambiguity Functions for Spatially Coherent and Incoherent Multistatic Radar," , *IEEE Trans on AES*, vol.46, no.1, pp.230-245, Jan. 2010